arXiv:nucl-ex/0201011v2 8 Mar 2002

The ^{3}He(e, e′d)p Reaction in (q, ω)-constant Kinematics

C.M. Spaltro [a,b,1], Th.S. Bauer [b,c], H.P. Blok [a,b], T. Botto [b], E. Cisbani [d], R. De Leo [e], G.E. Dodge [a,b], R. Ent [g], S. Frullani [d], F. Garibaldi [b], W. Glöckle [h], J. Golak [h,i], M.N. Harakeh [f], M. Iodice [d], E. Jans [b], H. Kamada [j], W.J. Kasdorp [b], C. Kormanyos [a,b], L. Lapikás [b], A. Misiejuk [b,c], S.I. Nagorny [a,b], G.J. Nooren [b], C.J.G. Onderwater [a,b], R. Perrino [e], M. van Sambeek [a,b], R. Skibiński [i], R. Starink [a,b], G. van der Steenhoven [b], J. Tjon [c], M.A. van Uden [b], G.M. Urciuoli [d], H. de Vries [b], H. Witała [i], and M. Yeomans [b,c]

[a] *Vrije Universiteit Amsterdam, de Boelelaan 1081, 1081 HV Amsterdam, The Netherlands*

[b] *Nationaal Instituut voor Kernfysica en Hoge-Energiefysica (NIKHEF), P.O. Box 41882, 1009 DB Amsterdam, The Netherlands*

[c] *Universiteit Utrecht, P.O. Box 80.000, 3508 TA Utrecht, The Netherlands*

[d] *INFN Sezione Sanitá, V.le Regina Elena 299, 00161 Roma, Italy*

[e] *INFN, Sezione di Lecce, via Arnesano, 73100 Lecce, Italy*

[f] *KVI, Rijksuniversiteit Groningen, Zernikelaan 25, 9747 AA Groningen, The Netherlands*

[g] *Thomas Jefferson National Accelerator Facility, Newport News, VA. 23606, USA*

[h] *Institut für Theoretische Physik II, Ruhr-Universität, D-44780 Bochum, Germany*

[i] *Institute of Physics, Jagellonian University, PL-30059 Cracow, Poland*

[j] *Kyushu Institute of Technology, 1-1 Sensuicho, Tobata, Kitakyushu 804-8550, Japan*

Abstract

The cross section for the ^{3}He(e, $e'd$)p reaction has been measured as a function of the missing momentum p_m in (q, ω)-constant kinematics at beam energies of 370 and 576 MeV for values of the three-momentum transfer q of 412, 504 and 604 MeV/c. The L(+TT), T and LT structure functions have been separated for q = 412 and 504 MeV/c. The data are compared to three-body Faddeev calculations, including meson-exchange currents (MEC), and to calculations based on

a covariant diagrammatic expansion. The influence of final-state interactions and meson-exchange currents is discussed. The p_m-dependence of the data is reasonably well described by all calculations. However, the most advanced Faddeev calculations, which employ the AV18 nucleon-nucleon interaction and include MEC, overestimate the measured cross sections, especially the longitudinal part, and at the larger values of q. The diagrammatic approach gives a fair description of the cross section, but under(over)estimates the longitudinal (transverse) structure function.

Key words:
PACS: 21.45+v, 25.10.+s, 25.30.Dh, 25.30.Fj

---

1 Introduction

Many nuclear properties can be described successfully within a mean-field approach. However, phenomena like the depletion of spectroscopic strength and the occurrence of bumps at missing energies characteristic of two-nucleon emission in $(e, e'p)$ reactions, indicate that correlations between nucleons, i.e., the motion inside a nucleus of two nucleons as a pair with a certain relative motion, also play an essential role. The $(e, e'd)$ reaction has proven to be a sensitive tool for the investigation of proton-neutron (pn) correlations in nuclei [1–7]. Assuming direct knock-out of a pn pair, the cross section for the $(e, e'd)$ reaction can approximately be written [6] as $d^6\sigma/dE_{e'}d\Omega_{e'}dE_d d\Omega_d = K\sigma_{e,pn}(q)S_{pn}(E_m, p_m, p_d)$. Here, the cross section $\sigma_{e,pn}$ for scattering of an electron from a pn pair leading to a deuteron in the final state, which depends on the momentum transfer q, reflects the relative proton-neutron motion, i.e., the relative pn wave function. The distorted spectral function S_{pn}, which depends on the missing energy E_m, the missing momentum p_m and the momentum of the final deuteron p_d, contains the information about the centre-of-mass (c.o.m.) motion of the pn pair within the nucleus, modified by final-state interactions (FSI). Since the deuteron has isospin zero and the initial pn pair can be in a $T = 0$ or $T = 1$ state, in general both $\Delta T = 0$ and $\Delta T = 1$ transitions are possible. The former resembles quasi-elastic knockout of a deuteron, whereas the latter is similar to the (inverse of) deuteron disintegration. Both types of transitions have been studied previously ([2,4–6], [3,6,7]).

In this paper we present data for the ^{3}He$(e, e'd)$ reaction, taken in so-called (q, ω)-constant kinematics, in which the energy and momentum transfer to the nucleus are held constant, while the angle of the outgoing deuteron is varied. The data is compared to the results of three-body calculations [8–10] and to

[1] present address: CMG, Graadt van Roggenweg 350, 3531 AH, Utrecht, The Netherlands

those of a covariant and gauge-invariant diagrammatic approach [11–14]. For the three-nucleon system Faddeev calculations are nowadays available both for the ground state and for the continuum. The first available ^{3}He(e, $e'd$) data [1] has been compared to the results of such calculations [8,10]. The emphasis in these calculations was on the correct treatment of FSI, which turned out to be crucial, especially for kinematics dominated by deuteron knock-out processes. The same data was also employed in Refs. [11–13], with the emphasis on the consistency between the dynamics and the one- and many-body currents. The agreement with the data, especially for parallel kinematics, was in both cases fairly good. Other data [7] was of limited kinematic coverage and no comparison to Faddeev calculations was made. More recently, we published data for the ^{3}He(e, $e'd$) reaction taken in parallel kinematics [15]. Theoretical calculations gave a fair description of the data, but there were some discrepancies, especially for the q dependence, and for the transverse structure function W_T.

Data in (q, ω)-constant kinematics extend the range in which the theoretical predictions can be tested, and feature some new aspects. First of all one can investigate the longitudinal-transverse (LT) interference structure function, which is more sensitive to details of the interaction currents. Furthermore, one can investigate the dependence of the longitudinal (L) and transverse (T) structure functions on the kinematics. Finally, in selected parts of this kinematics one gets non-negligible contributions from processes in which the photon hits the non-detected proton. Interference with the process where the photon interacts with (the nucleons of) the deuteron gives an extra sensitivity to a correct description of the reaction.

Since the publication of the data obtained in parallel kinematics there have been several theoretical developments (see section 3). The Faddeev calculations by Golak et al. [10] were extended by using the AV18 NN potential in addition to the Bonn-B potential, and by including meson-exchange currents (MEC). Furthermore, the number of partial waves was increased to ensure full convergence. New calculations in the diagrammatic approach by Nagorny [11–14] employed also the AV18 potential instead of the Reid Soft Core potential, and now include all angular momentum states in the ^{3}He ground state.

Since the data to be discussed comprise both the q and p_m dependence of the reaction, different aspects of the pn motion in the nucleus ^{3}He can be studied. Furthermore, the cross sections were measured at two beam energies, so that a separation of the longitudinal (W_L) plus transverse-transverse (W_{TT}), transverse (W_T), and longitudinal-transverse interference (W_{LT}) structure functions could be performed.
For the definition of the structure functions we follow Raskin and Donnelly [16], who write the differential cross section for the unpolarized $(e, e'd)$ reaction

as:

$$\frac{d^5\sigma}{dE_{e'}d\Omega_{e'}d\Omega_d} = C\ (v_L W_L + v_T W_T + v_{LT} W_{LT}\cos\phi + v_{TT} W_{TT}\cos 2\phi), \quad (1)$$

where ϕ is the angle between the electron scattering plane and the plane defined by the momentum transfer $\vec{q}$ and the momentum of the outgoing deuteron $\vec{p_d}$. The factor C contains the Mott cross section and kinematical factors. Its precise form, as well as that of the kinematical factors v_i, are given in Ref. [16]. The structure functions W_{LT} and W_{TT} are zero in parallel kinematics.

The separate structure functions, which result from different combinations of the components of the nuclear current, have a different sensitivity to the various aspects of the reaction. For instance, the coupling of the virtual photon to a $T = 1$ pn pair, transforming it into a deuteron, involves a spin-flip and thus is purely transverse, whereas the coupling to an initial $T = 0$ pair, which resembles elastic $e-d$ scattering, is dominantly longitudinal at our values of q (see also [3,7]). Furthermore, one expects that MEC will mainly contribute to W_T. On the other hand, according to the three-body calculations the effects of FSI on W_L are quite different from the ones on W_T.

2 Experiment

The ^{3}He$(e,\ e'd)p$ reaction has been measured "in-plane", using $(q,\ \omega)$-constant kinematics, for missing momenta up to 210 MeV/c, and for values of the transferred momentum q of 412, 504 and 604 MeV/c. The (central) kinematics is given in Table 1. In later figures a negative sign of p_m denotes kinematics in

Table 1
Overview of the kinematics. $T_{\rm cm}$ denotes the centre-of-mass energy of the outgoing deuteron.

q (MeV/c)	ω (MeV)	$T_{\rm cm}$ (MeV)	$\theta_{e'}$ (576 MeV) (deg.)	$\theta_{e'}$ (370 MeV) (deg.)
412	50.0	14.7	43.6	72.9
504	70.0	21.0	55.1	97.0
604	100.0	31.1	69.3	-

which $\theta_d < \theta_q$ (corresponding to $\phi = 0$ in Eq. 1), and a positive p_m kinematics with $\theta_d > \theta_q$ (corresponding to $\phi = \pi$ in Eq. 1).

Since the experiment has been described in detail in Refs. [17,18], only the main points are mentioned here.

The experiment was performed with the extracted electron beam from the pulse-stretcher ring AmPS [19] at NIKHEF. The beam energies were 370 and 576 MeV. The extracted electron current was about 6 μA and had a duty factor of about 70%. The scattered electrons were detected with the QDD spectrometer and the knocked-out deuterons with the QDQ spectrometer [20].

A cryogenic gas target [21] operating at 20 K and 1.5 Mpa was used, which was filled with a mixture of ^{3}He and ^{4}He gases. In this way data was collected simultaneously for the three reactions: ^{3}He(e, $e'd$)p, ^{4}He(e, $e'd$)d and ^{4}He(e, $e'd$)pn. Results on the latter reaction channel have been published separately [18].

The resolution in missing energy varied between 0.3 and 2.0 MeV, depending on the kinematics, which was sufficient to separate the different reaction channels. The absolute ^{3}He and ^{4}He target thicknesses were determined by comparison of the measured elastic scattering cross sections to calculated ones [22,23]. During the $(e, e'd)$ measurements the total target thickness was monitored through the singles rate of either one of the spectrometers. Checks with elastic scattering before and after each set of $(e, e'd)$ measurements were consistent to within 2%.

Both the ^{2}H$(e, e'd)$ and the ^{1}H$(e, e'p)$ reaction were used in order to check the reconstruction of the electron and hadron momentum vectors in the QDD and QDQ spectrometers and to determine the coincidence detection efficiency.

The data analysis included the following steps. First, the deuterons were separated from protons and tritons by using the pulse height from the scintillators in the QDQ spectrometer. Next, the particle vectors at the target were reconstructed. Since an extended target was used, this reconstruction and the acceptances of both spectrometers depend on the position of the interaction point along the beam. By using energy and momentum conservation the values of the missing energy

$$E_m = \omega - T_p - T_d, \tag{2}$$

where T_x is the kinetic energy of particle x, and the missing momentum

$$p_m = \vec{q} - \vec{p_d} \tag{3}$$

were calculated from the particle vectors. Next, the accidental coincidences were subtracted. As a result of the high duty-factor of the extracted beam, the real-to-accidental ratio was high, ranging from 15 to 1640 depending on

the kinematics. Next, the data was normalised to the target thickness, the integrated charge and the experimental detection volume, and corrected for detection inefficiencies. The detection volume was obtained from a Monte-Carlo simulation, which uses the measured optical properties of the spectrometers [24–26], including their vertex-position dependent angular acceptances. Finally, the data was radiatively unfolded. The systematic uncertainty amounts to about 3% for the cross sections and 4-5% for the structure functions [17,18].

The cross section measured in one kinematical setting covers an appreciable range in p_m, as a consequence of the angular and momentum acceptances of the spectrometers. However, over this range the values of q and the kinematical factors in the cross-section expression of Eq. (1) vary slightly around the central values. A Monte-Carlo simulation was performed to determine the average values of the kinematical factors and of q for the different p_m bins within one measurement. Then, the cross sections for the different p_m bins were recalculated to a common q value by using the q dependence of the cross section as measured in this experiment. The correction to the cross section amounted to typically a few percent.

3 Theoretical calculations

The experimental data is compared to the calculations of Van Meijgaard and Tjon [8], Golak et al. [9,10,27] and Nagorny et al. [13,14]. The results of Van Meijgaard and Tjon are based on solutions of the Faddeev equations for the three-body system, employing a central local NN-interaction, the spin-dependent Malfliet-Tjon I-III potential [28], in the Unitary Pole Expansion (UPE). Since this interaction contains only s-wave forces, the ground-state wave function of ^{3}He includes only s-waves. Furthermore, a relativistic current operator is used.

The calculations of Golak et al. are also based on the solution of Faddeev-like equations, but employ the one-boson-exchange Bonn-B potential [29] and the AV18 interaction. [30]. Thus state-of-the-art ^{3}He and 3N continuum wave functions are employed. A non-relativistic single-nucleon current operator is used, consistent with the non-relativistic Schrödinger equation for the 3N states. (The lowest-order relativistic corrections to the single-nucleon density operator were studied and found to be on the 5% level in the range of small p_m values.) In addition π- and ρ-like exchange currents [31] are included, which in case of the AV18 potential are consistent with the forces. The Riska prescription [32] was employed, which guarantees that the currents fulfill the continuity equation. In this approach the transverse currents j_x and j_y explicitly include MEC, while j_z is related to the charge current j_0 through the

continuity equation. MEC were not included in the charge density operator. This would be a relativistic effect, which was not considered. In case of the Bonn-B potential standard [33] π- and ρ-like exchange currents are taken. The electromagnetic nucleon form factors used are the ones from Hoehler et al. [34].

Nagorny et al. use quite a different approach, which is based on including the electromagnetic field into the strongly-interacting system in a fully relativistic and gauge-invariant way [11]. Two covariant sets of diagrams, including pole, "contact" and one-loop diagrams are used, which provide both nuclear-current conservation and inclusion of the dominant part of FSI and MEC effects in a form that is consistent with the nuclear dynamics. The diagrams were generated by "minimal insertion" of the electromagnetic field into all external/internal lines and also directly into the 3- and 4-point nuclear vertices, which produces various contact currents in accordance with Ward-Takahashi identities [12]. The strong form factors in the covariant nuclear vertices ^{3}He$\rightarrow pd$ and ^{3}He$\rightarrow ppn$ are taken as the positive-energy states in the laboratory frame through the solutions of the Faddeev equations with the AV18 potential. All angular momentum states in the ground state of ^{3}He are included. The electromagnetic form factors in the completely relativistic γNN-, γdd- and γ^3He^{3}He-vertices are taken from standard parameterizations of experimental form factors.

4 Results

4.1 Direct proton knock-out

We first focus on the measurements at $q = 412$ MeV/c at the higher beam energy, where the largest range in p_m has been probed. The measured ^{3}He(e, $e'd$) cross sections for this kinematics are shown in Fig. 1. Above a certain value of p_m the cross section flattens off, an effect that is not seen in parallel kinematics [15]. The origin of this effect can easily be understood. If one neglects FSI the virtual photon can either couple to the proton that is knocked out, while the detected deuteron acts as a spectator (direct proton knock-out: DPKO), or the virtual photon couples to either one of the nucleons that constitute the final deuteron, which is knocked out, while the proton is a spectator (direct deuteron knock-out: DDKO). Inclusion of FSI modifies this picture quantitatively, but not qualitatively.

Now one can look into the kinematics. In the case of DDKO, p_m and (the constant value of) q combine to the detected deuteron momentum p_d, which decreases from about 400 MeV/c at $p_m = 0$ MeV/c to about 340 MeV/c at

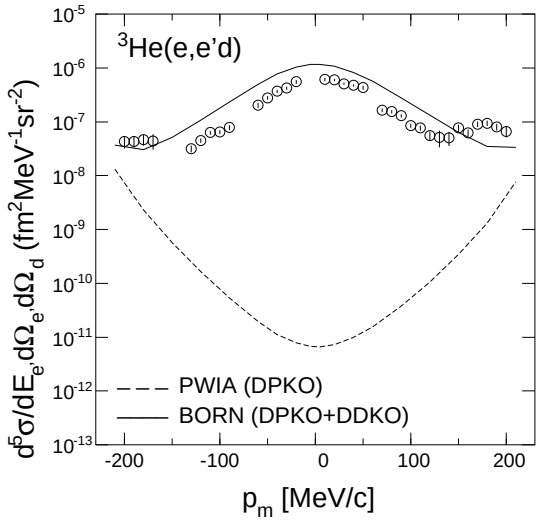

Fig. 1. Measured cross sections for the ^{3}He(e, $e'd$) reaction for q = 412 MeV/c at E_e = 576 MeV. The curves are the PWIA (dashed line) and BORN (full line) calculations of Tjon et al., showing the competition between DPKO and DDKO.

p_m = 200 MeV/c. However, in case of DPKO the effective p_m is equal to p_d. Since for both processes the cross section decreases with the effective value of p_m, the cross section is dominated at low p_m by DDKO, but for increasing p_m values the contribution of DPKO increases.

Although for a quantitative comparison with the data the effects of distortions have to be included, the PWIA and BORN calculations of Van Meijgaard and Tjon show this nicely. The PWIA calculation contains only the DPKO term, while the BORN calculation includes both the DPKO and the DDKO contribution. Whereas for $p_m = 0$ the PWIA calculation is orders of magnitude below the data, it increases rapidly with p_m, ending up only one order of magnitude below the data at the largest values of p_m measured. The BORN calculation is largest around $p_m = 0$ and then decreases, but flattens off at large p_m values due to the increasing contribution of the DPKO part.

4.2 Cross sections

Before discussing all data and the comparison with the calculations, it is of interest to look into the influence of final-state interactions (FSI). The ratio of the FULL cross sections, i.e., including FSI, over the ones calculated in PWIAS, which means a fully antisymmetrized plane-wave impulse approximation [10] (equivalent to the BORN cross section by Van Meijgaard and Tjon), is shown in Fig. 2. One observes that FSI effects around $p_m = 0$ decrease the cross section considerably at q = 412 MeV/c, but less so at larger q. This has already been noticed before [10]. Here, one should keep in mind that the $p - d$ centre-of-mass energy is only 14.7 MeV at the lowest q-value, rising to

31.1 MeV at the highest q-value. In the latter case the reduction of the cross section at low values of p_m is already rather small, about 10-15%. Beyond a $|p_m|$-value of about 150 MeV/c FSI increases the cross section considerably. (Overall the effects are slightly smaller at the lower electron energy. We will come back to this later when discussing the separated structure functions).

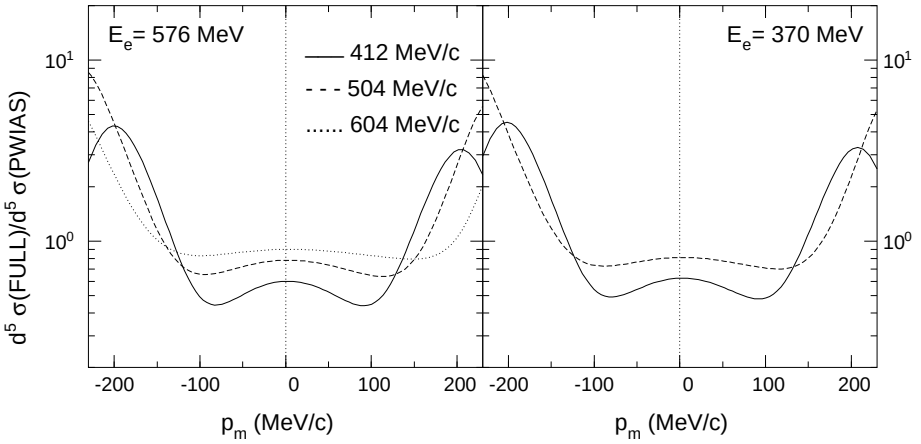

Fig. 2. Ratio of FULL and PWIAS cross sections as calculated by Golak et al. with the AV18 potential, for different values of the momentum transfer.

The measured $(e, e'd)$ cross sections for the various kinematics are shown in Fig. 3. Since the calculations of Golak et al. are the most detailed, we will first compare those to the data. One can make three observations. The first one is that the calculations overestimate the data. This holds already for the results with the Bonn-B potential, and even more for the AV18 ones. The inclusion of MEC increases the discrepancy. Secondly, the (relative) difference between data and calculations is slightly smaller at the lower beam energy (we will discuss this further in the next subsection) and increases with q. Finally, the p_m dependence of the data is fairly well described, except at $q = 412$ MeV/c, where there is a discrepancy at negative p_m, in the region where the cross section flattens off due to the influence of DPKO. Obviously the interference between the DPKO and DDKO processes is not well described.

In Fig. 4 the three theoretical approaches are compared with each other and with the data. For the calculations by Golak et al. the AV18 results are chosen, since these forces and the accompanying MEC are considered to be the most realistic ones. In addition to what has been said already about the various calculations some more points are worth mentioning.

It is seen, especially at small p_m-values, that with increasing values of q the calculations by Van Meijgaard and Tjon predict increasingly smaller values for the cross section compared to those calculated by Golak et al.. Since in first approximation the q-dependence of the cross section probes the wave function of the pn-pair, part of this may reflect the increasing importance of the D-

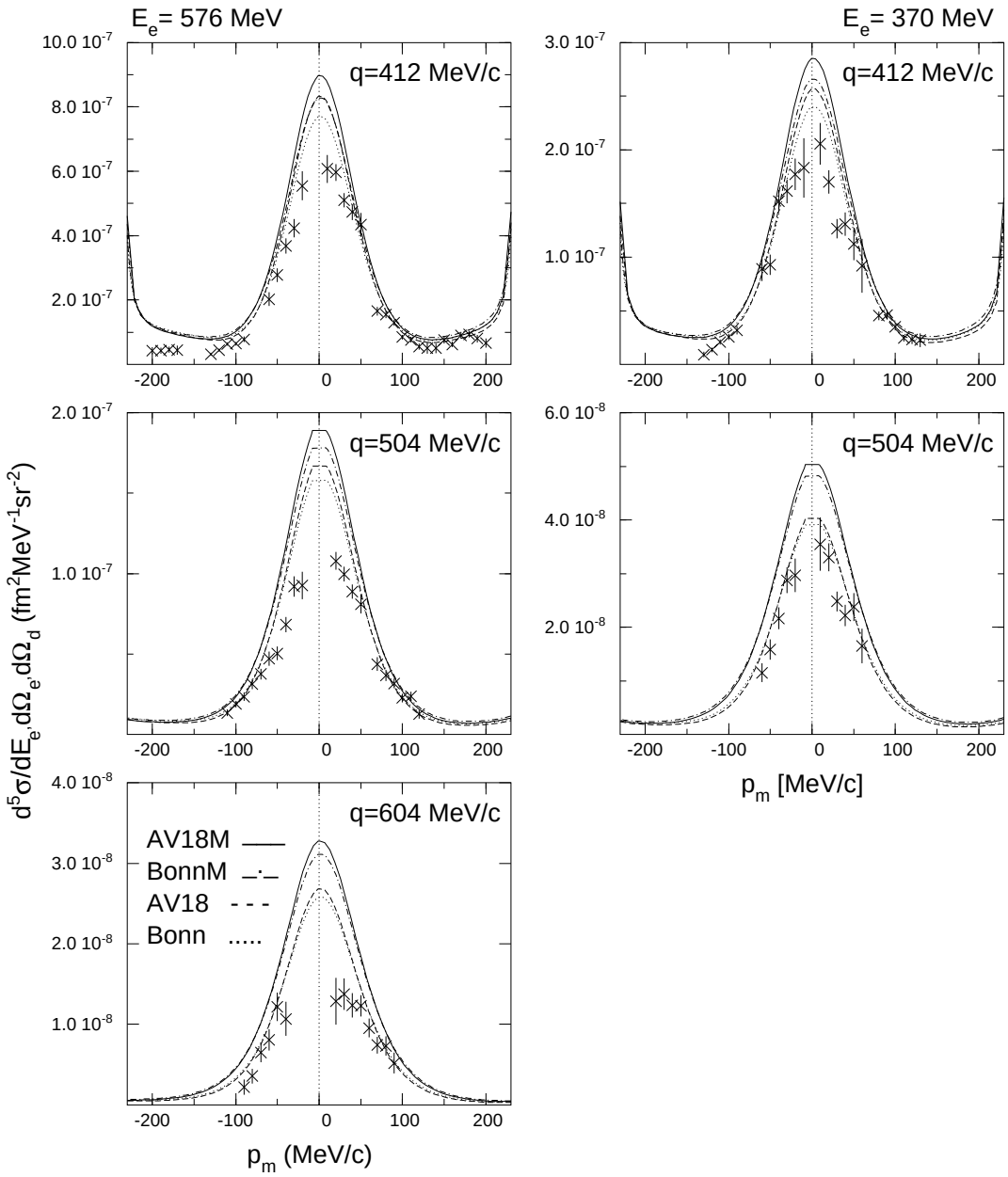

Fig. 3. Measured cross sections for different values of q at the two beam energies, compared to the results of the calculations by Golak et al. for the Bonn-B (dotted and dash-dotted curves) and AV18 potential (dashed and full curves), without and with the inclusion of MEC, respectively.

state of the pn-pair (compare elastic scattering from the deuteron at these q-values [35]). As mentioned, the calculations by Van Meijgaard and Tjon do not contain d-waves. Golak et al. have also performed calculations with the MT I-III potential, using their non-relativistic single-nucleon current. The results agree quite well with the ones by Van Meijgaard and Tjon.

The calculations by Nagorny give a fairly good description of the data. At $q = 412$ MeV/c earlier calculations [17] were significantly lower than the data

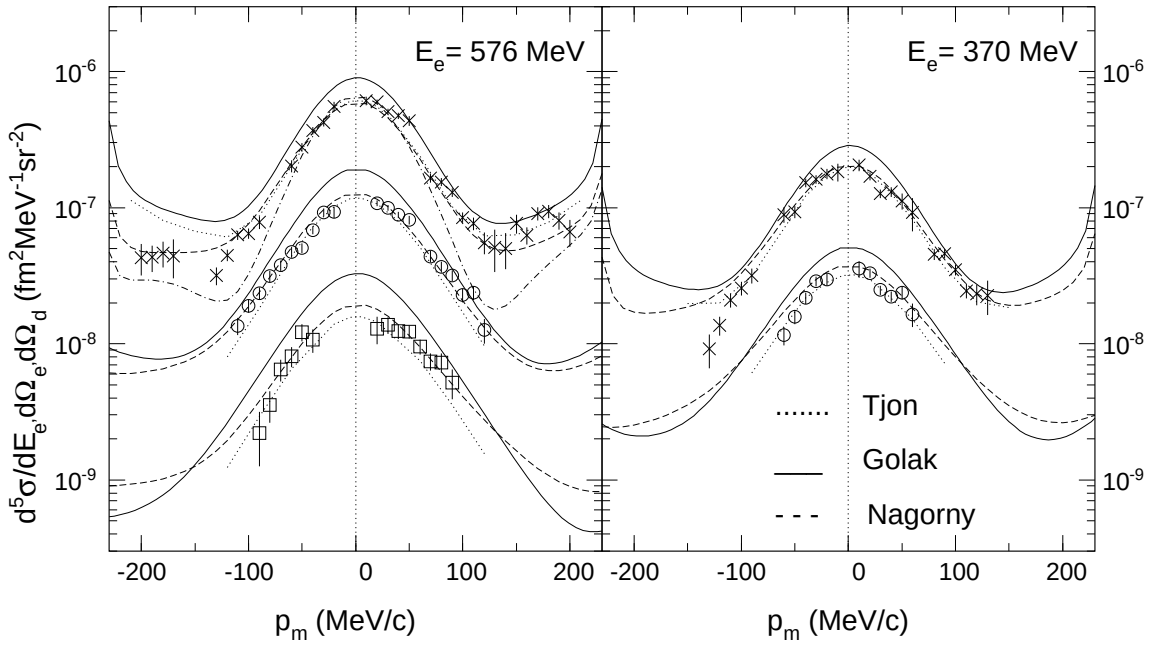

Fig. 4. Measured cross sections at both electron energies for the different values of q: 412 MeV/c (crosses), 504 MeV/c (circles) and 604 MeV/c (squares). The data is shown together with the FULL calculations of Van Meijgaard and Tjon (dotted line), Golak et al. (full line) and Nagorny (dashed line). See the text for the dash-dotted line.

for p_m >100 MeV/c (see the dash-dotted line in Fig. 4). In contrast to those the present calculations include also the $l = 2, L = 2$ configuration in the ^{3}He ground state. Although this component is small, it has a relatively large influence at larger values of p_m due to its overlap with the deuteron $l = 2$ (D) state. Altogether, these calculations give a fairly good description of both the p_m- and the q-dependence of the data.

4.3 Structure functions

As mentioned in section 2, the experimental data was obtained for values of ϕ close to 0 and π, and for two values of the incoming electron energy, so the structure functions $W_L + \frac{v_{TT}}{v_L} W_{TT}$, W_T and W_{LT} (see Eq. 1) could be separated.

Before discussing the data it is instructive to look at the theoretical predictions. In Fig. 5 the separate structure functions at $q = 412$ MeV/c calculated by Golak with the AV18 interaction, with and without inclusion of FSI and MEC, are shown. It is clear that W_L and W_T are the dominant structure functions, and that W_T is not small compared to W_L. This is due to the contribution of the (fully transverse) $\Delta T = 1$ transition (the $\Delta T = 0$ transition is dominantly longitudinal), see Refs. [7,18]. The W_{LT} interference structure function is rather small, while W_{TT} is negligible except for values of p_m above

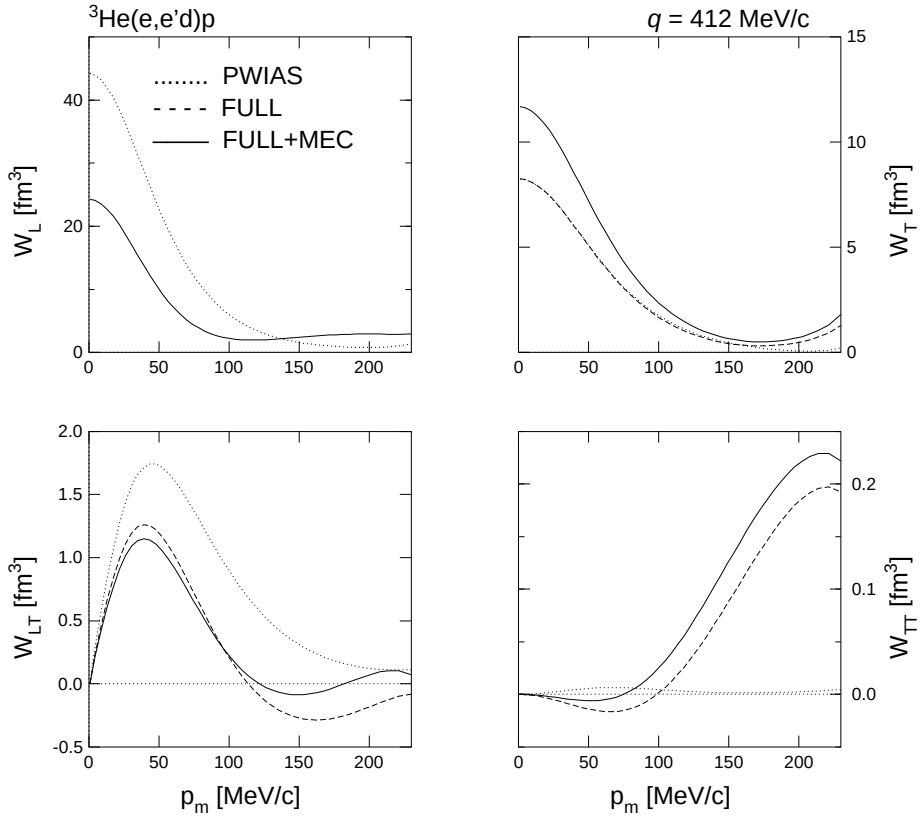

Fig. 5. Structure functions calculated by Golak et al. with the AV18 potential for $q = 412$ MeV/c. Notice the different vertical scales for the different W's.

about 150 MeV/c.
Another interesting observation is that the influence of FSI is large in W_L (and in W_{LT} and W_{TT}), but very small in W_T, except at large values of p_m. In this context one should realize that a PWIAS calculation for W_L violates current conservation. On the other hand MEC, as included in the present approach, only influence the 'transverse current' dependent W's, considerably increasing the values of W_T and W_{TT}.

W_{LT}

The W_{LT} structure function can be determined by just comparing the data in kinematics with θ_d smaller and larger than θ_q (see section 2). The separated W_{LT} structure functions for the three values of q are shown together with the calculations in Fig. 6, both for E_e= 576 MeV and E_e= 370 MeV. The values obtained at the two different energies agree within the experimental uncertainties. As is already clear on the cross section level, where the difference between the data for θ_d smaller and larger than θ_q is not very large, the measured W_{LT} is small, so the error bars are relatively large. The theoretical curves for W_{LT} were obtained by separating the calculated cross sections in the same way as the measured cross sections. (Naturally they agreed with the ones calculated directly, using the appropriate components of the hadronic

current operator). For all calculations W_{LT} is independent of the incoming energy, as expected, and has a maximum near p_m= 50 MeV/c for all q values, while it decreases for higher p_m values. In the Faddeev calculations FSI has two effects on W_{LT}: both the magnitude of the maximum decreases and the decrease as a function of p_m is stronger. This even introduces a zero crossing at q= 504 MeV/c and a double zero crossing at q= 412 MeV/c. The latter presumably is related to the increasing influence of DPKO, which is also visible in this region in the cross section.
In the p_m range between 0 and about 70 MeV/c the data and the various calculations agree with each other within the experimental accuracy. However, at larger values of p_m the calculations tend to underestimate the data.

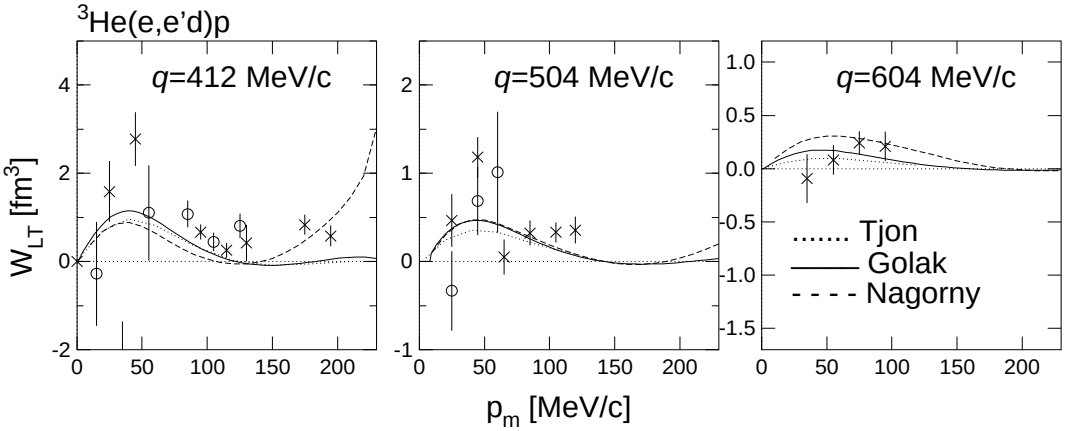

Fig. 6. Measured W_{LT} structure functions, extracted from the cross sections measured at E_e=576 MeV (crosses) and E_e=370 MeV (circles), for the different q values, in comparison to the calculations.

W_L and W_T

Data at q= 412 MeV/c and q= 504 MeV/c were taken at both energies. Therefore, for the first time the $W_L(+\frac{v_{TT}}{v_L}W_{TT})$ and W_T structure functions could be separated in (q, ω) kinematics, for those p_m values where all four cross sections were available. Since all calculations predict W_{TT} to be very small compared to W_L, except at values of p_m above about 150 MeV/c, this is effectively an L-T separation. The results are presented in Fig. 7. It turns out that the values found for W_L and W_T in (q, ω) kinematics are very close to the values found in parallel kinematics [15]. This, together with the fact that W_{LT} and W_{TT} are small, suggests that a factorization of the cross section into an '$e-pn$' cross section and a (distorted) spectral function (see also the introduction and Ref. [6]) is a reasonable approximation.

The calculations by Golak et al. with the AV18 potential and including MEC are in global agreement with W_T, but overestimate W_L, especially at q = 504 MeV/c. In this context we recall that at q = 604 MeV/c, where no separation of the structure functions could be performed, the unseparated cross

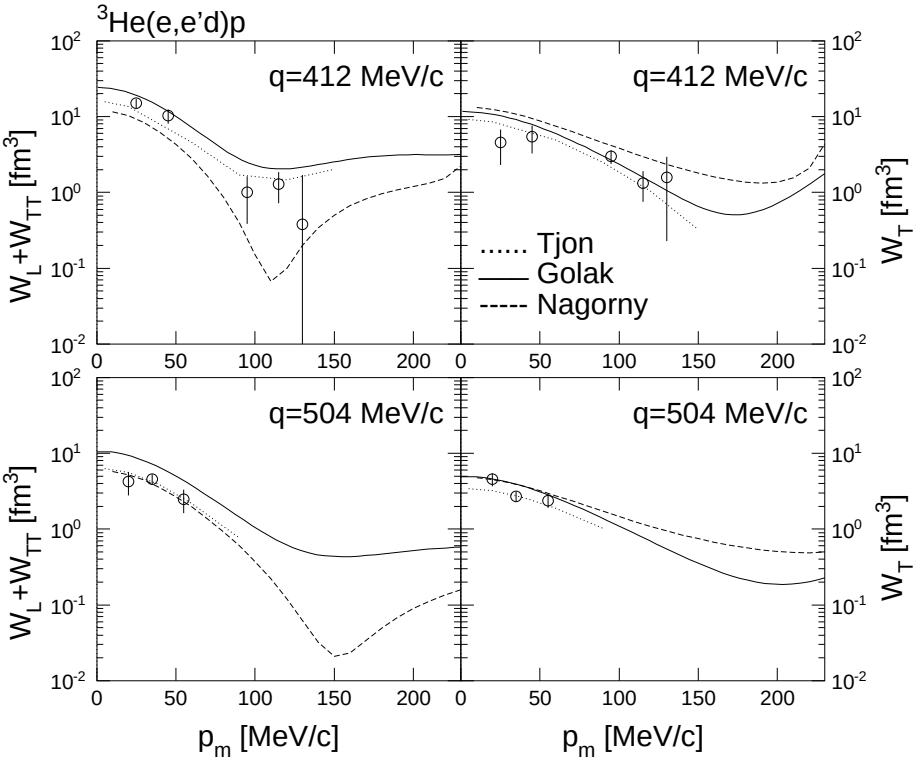

Fig. 7. Data for the structure functions W_L $(+W_{TT})$ and W_T together with the results of the calculations.

section was even more overestimated. Since the q-dependence in first instance probes the relative motion of the pn pair in ^{3}He, this suggests that the short-distance behaviour of this motion is not well described. (As the used current operator is a non-relativistic one, it was verified that elastic scattering from the free deuteron was well described).

Whereas the calculations by Nagorny gave a fairly good description of the measured cross sections, they clearly underestimate the longitudinal structure function W_L at $q = 412$ MeV/c, and overestimate W_T. The calculations show a minimum for W_L, which is not present in a PWIAS calculation. This has been observed before by Nagorny et al. [13]. The cause is a large, destructively interfering, contribution of the ^{3}He-pole diagram (S-term) in (q, ω) kinematics. This term, which is part of the FSI, is constant with p_m, since it only depends on ω. Another part of the FSI comes from the "contact current", but this part is still small at $q = 412$ MeV/c. Clearly, this indicates an inadequacy of the treatment of FSI. Presumably, inclusion of only the pole part of $pd \rightarrow pd$ rescattering is not sufficient, and the regular part [12] has to be included as well.

Although the pioneering calculations by Van Meijgaard and Tjon give a reasonable description of the data, this observation does not allow strong conclusions, since the used interaction is rather simple, no MEC are included, and

only s-waves are taken into account.

5 Summary and conclusions

Cross sections for the ^{3}He$(e, e'd)p$ reaction have been measured in (q, ω)-constant kinematics for a range in missing momentum at two beam energies and for three values of the three-momentum transfer. Thus the separate L(+TT), T and LT structure functions could be determined at $q = 412$ and 504 MeV/c, which provide for a sensitive test of theoretical calculations for this reaction. The LT structure function is found to be rather small, but the transverse structure function is of comparable magnitude as the longitudinal one. This points to the importance of the $\Delta T = 1$ transition, in which a $T = 1$ pn pair in ^{3}He is transformed into a $T = 0$ deuteron in the final state.

The data has been compared to the results of two types of three-body Faddeev calculations, one with a simple interaction and containing only s-waves, the other one employing the Bonn-B and the AV18 potentials, and including meson-exchange currents (MEC). Also calculations based on a covariant diagrammatic approach, including tree and one-loop diagrams, and using Ward-Takahashi identities to ensure gauge invariance were used.

All calculations give a fair description of the p_m- and the q-dependences of the cross sections, which reflect the centre-of-mass and relative motion of the pn pair inside ^{3}He, respectively, and of their L/T character. This means that the essential ingredients of the calculations: the structure of ^{3}He in its ground state, and final-state interactions (the continuum structure of the 3N system), are reasonably well understood. Final-state interactions have a large influence, especially at the lower value of q (and accompanying low centre-of-mass energy of the final p-d system). At low values of p_m they reduce the longitudinal part of the cross section, whereas at large p_m-values they increase it. In this region also direct proton knock-out starts to noticeably influence the cross sections, leading to a rise of the cross section. This was experimentally observed at p_m-values above 150 MeV/c at the lowest value of q. In contrast the value of the transverse structure function hardly changes when including FSI. Meson-exchange currents increase considerably the transverse structure function. All calculations predict relatively small values for the LT interference structure function, which is consistent with the data. Also W_{TT} is calculated to be small, but this structure function cannot be separated with the present "in-plane" data.

However, upon closer inspection there are also significant differences between the data and the theoretical calculations. The diagrammatic approach gives a fair description of the cross section, but under(over)estimates the longitudinal

(transverse) structure function. It also predicts a minimum in the longitudinal structure function, presumably due to the neglect of the regular part of $pd \to pd$ rescattering. The most striking result is that the supposedly best Faddeev calculations available at present, which employ the AV18 nucleon-nucleon interaction and include MEC, overestimate the measured cross sections, the more the larger the value of q. The major discrepancy is in the longitudinal cross section, the transverse one being reasonably well described. Possible explanations for this discrepancy could be: the use of the Sachs form factors G_E^p and G_E^n instead of the Pauli form factors F_1^p and F_1^n reduces the longitudinal response function R_L by about 15-25%, depending on the kinematics. Furthermore, inclusion of a three-nucleon force will influence the binding energy and hence the $d-p$ overlap. A PWIAS calculation including the Urbana IX 3N force [36] for the ^{3}He bound state gives a reduction of the cross section of about 15%. Finally meson-exchange currents should also be included in the charge-density operator, since it is known that they influence e.g. the elastic charge form factor. However, such calculations are not yet available.

Acknowledgements

This work is part of the research programme of the "Stichting voor Fundamenteel Onderzoek der Materie (FOM)", which is financially supported by the "Nederlandse Organisatie voor Wetenschappelijk Onderzoek (NWO)". The Faddeev calculations by Golak et al. were supported by the Deutsche Forschungsgemeinschaft and the Polish Committee for Scientific Research. The calculations were performed on the T90 of the NIC in Jülich.

References

[1] P.H.M. Keizer *et al.*, Phys. Lett. **157B**, 255 (1985).

[2] R. Ent *et al.*, Phys. Rev. Lett. **57**, 2367 (1986).

[3] R. Ent *et al.*, Phys. Rev. Lett. **62**, 24 (1989).

[4] R. Ent *et al.*, Phys. Rev. Lett. **67**, 18 (1991).

[5] M. Iodice *et al.*, Phys. Lett. **B282**, 31 (1992).

[6] R. Ent *et al.*, Nucl. Phys. **A578**, 93 (1994).

[7] C. Tripp *et al.*, Phys. Rev. Lett. **76**, 885 (1996).

[8] E. van Meijgaard and J.A. Tjon, Phys. Rev. C **42**, 74 and 96 (1990).

[9] S. Ishikawa *et al.*, Nuovo Cimento **107A**, 305 (1994).

[10] J. Golak *et al.*, Phys. Rev. C **51**, 1638 (1995).

[11] S.I. Nagorny *et al.*, Sov. J. Nucl. Phys. **49**, 465 (1989).

[12] S.I. Nagorny *et al.*, Sov. J. Nucl. Phys. **53**, 228 (1991).

[13] S.I. Nagorny, Yu.A. Kasatkin and V.A. Zolenko, Phys. At. Nucl. **57**, 940 (1994).

[14] S.I. Nagorny, in *Few-Body Problems in Physics*, edited by F. Gross, AIP Conf. Proc. No 33 (AIP, Williamsburg, 1994), p. 757.

[15] C.M. Spaltro *et al.*, Phys. Rev. Lett. **81**, 2870 (1998).

[16] A.S. Raskin and T.W. Donnelly, Ann. Phys. (N.Y.) **191**, 78 (1989).

[17] C.M. Spaltro, Thesis Vrije Universiteit, Amsterdam, 1997

[18] C.M. Spaltro *et al.*, Few-Body Systems **26**, 271 (1999).

[19] P.K.A. de Witt Huberts, Nucl. Phys. **A553**, 845c (1993).

[20] C. de Vries *et al.*, Nucl. Instr. Meth. **223**, 1 (1984).

[21] O. Unal, PhD thesis, University of Wisconsin, 1995 (unpublished); see also H.B. van den Brink *et al.*, Nucl. Phys. **A612**, 391 (1997).

[22] A. Amroun *et al.*, Nucl. Phys. **A579**, 596 (1994).

[23] H. de Vries, C.W. de Jager and C. de Vries, At. Data Nucl. Data Tables **36**, 495 (1987).

[24] H. Blok *et al.*, Nucl. Instr. Meth. **A262**, 291 (1987).

[25] E.A.J.M. Offermann *et al.*, Nucl. Instr. Meth. **A262**, 298 (1987).

[26] L. de Vries *et al.*, Nucl. Instr. Meth. **A292**, 629 (1990).

[27] V.V. Kotlyar *et al.*, Few-Body Systems **28**, 35 (2000).

[28] R.A. Malfliet and J.A. Tjon, Nucl. Phys. **A127**, 391 (1969).

[29] R. Machleidt, Adv. Nucl. Phys. **19**, 189 (1989).

[30] R.B. Wiringa, V.G.J. Stoks, R. Schiavilla, Phys. Rev. **C51**, 38, 1995

[31] J. Carlson and R. Schiavilla, Rev. Mod. Phys. **70**, 743 (1998).

[32] D. O. Riska, Phys. Scr. **31**, 107 and 471 (1985).

[33] J.-F. Mathiot, Phys. Rep. **173**, 63 (1989).

[34] G. Hoehler *et al.*, Nucl. Phys. **B114**, 1638 (1995).

[35] T. de Forest, Phys. Rev. C **54**, 646 (1996).

[36] B. S. Pudliner *et al.*, Phys. Rev. C **56**, 1720 (1997).